**REGULAR ARTICLE**

# Investigation of Dynamic-Mechanical-Thermal Analysis of Innovative Hybrid Carbon/Glass Fibers Reinforced by GNPs and Al$_2$O$_3$ for Marine Structures

Mohamed Abu-Okail[1] · Metwally Abdel Ghafaar[1] · Abou Bakr Elshalakany[2,3] · Mohamed S. Shiba[4] · Ahmed Abu-Oqail[5] · Mohammed Gamil[6]

**Abstract**

Marine structural applications face numerous challenges related to environmental load, corrosion, and fatigue under varying time and temperature conditions. One of the major challenges faced by marine structural applications is dynamic mechanical thermal analysis (DMTA). In this study, innovative hybrid carbon/glass fibers (CGF) reinforced with different contents (1.5 wt. % and 3 wt. %) of dual nano-powders, including graphene nanoplatelets (GNPs) and aluminium oxide (Al$_2$O$_3$), were developed as reinforcements inside the epoxy matrix. The nanocomposites were fabricated using a hand lay-up technique, resulting in a nanocomposite sheet with dimensions of 300 mm length, 200 mm width, and 2.3 mm thickness. DMTA test specimens were prepared with dimensions of 50 mm length, 10 mm width, and 2.3 mm thickness. To ensure accuracy, three replicates were conducted for each condition, and the average values were calculated for analysis. Before DMTA, the prepared nanocomposites were analyzed using optical microscopy (OM), scanning electron microscopy (SEM), and energy-dispersive X-ray spectroscopy (EDAX) to compare the influence of incorporating dual nano-powders. DMTA was carried out at different temperature values (ranging from 10 °C to 105 °C) and times (ranging from 5 to 575 min) at 1 Hz frequency with a heating rate of 4 °C/min and a nitrogen flow rate of 20 ml/min. The main objective of this study was to investigate the influence of incorporating dual nano-powders such as GNPs and Al$_2$O$_3$ on various dynamic mechanical properties including storage modulus, loss modulus, damping factor (DF), and glass transition temperature (Tg) of the hybrid carbon/glass fiber-reinforced epoxy composites. The fabricated hybrid CGF composite with 1.5% wt. GA nanoparticles exhibited higher values for the DF of 0.68 and the Tg of 73.4 °C. However, increasing the nanoparticle content to 3% wt. GA led to a deterioration in the DF (0.54) and a reduction in Tg (27.8 °C) due to decreased bonding between the carbon fibers (CF) and glass fibers (GF) caused by the higher nanoparticle concentration. The complex modulus (E*) values demonstrated expected trends with temperature and time for the CGF-1.5% wt. GA composite, indicating acceptable behaviour. In contrast, the CGF-3% wt. GA composite exhibited lower E* values, indicating a decrease in stiffness and mechanical properties compared to the CGF-1.5% wt. GA composite. Microstructural observations after DMTA revealed a uniform scattering of nanoparticles in the CGF-1.5% wt. GA sample, while the CGF-3% wt. GA sample demonstrated improved scattering of Al$_2$O$_3$ nanoparticles on the surface. The microstructural analysis further indicated a brittle nature with high resistance to crack initiation and propagation in the CGF-1.5% wt. GA composite.

**Keywords** Dual nano-powders (GNPs and Al$_2$O$_3$) · Dynamic mechanical thermal analysis (DMTA) · Dynamic mechanical properties · Marine structural applications

## 1 Introduction

Marine structures face significant challenges from environmental loads, corrosion, and fatigue [1–3]. These structures come in various designs, including (i) submersibles, (ii) floating platforms, (iii) offshore installations, and (iv) watercraft. To meet the demanding requirements, composite

materials have emerged as the most suitable choice [4]. Among the composites, fiber-reinforced polymers (FRPs), such as GF, CF, and aramid, stand out for their lightweight, high strength, corrosion resistance, and fatigue performance [5, 6]. The use of FRPs as functional graded materials, with varying fiber intensity, allows for tailored strength distribution based on part function. Hybrid structures combining FRPs with CGF have been proposed as a cost-effective means to achieve unique properties [7]. These materials must possess: (i) high-strength-to-weight ratio, (ii) good fracture toughness, and (iii) excellent fatigue strength, to ensure design requirements and reliability [8].

Hybrid composite materials find application in various marine structures, including hull shells, piping, hatch covers, ducts, gratings, sonar domes, vessels, propellers, bearings, and topside structures [9]. To enhance stiffness and strength while maintaining lightweight, marine industries commonly use composite sandwich structures, consisting of two skins and a soft, thick core [10–12].

The skins, made of materials like glass, carbon, or aramid, handle bending stress, while the cores, composed of polystyrene, PVC, honeycomb, etc., handle shear and compression stress [13–15]. Weight reduction is crucial for improving ship stability, fuel efficiency, buoyancy, and cargo capacity [16], and corrosion resistance reduces maintenance needs [17]. Although FRPs used in hybrid structures offer high strength, they face challenges such as delamination, low fatigue resistance, and high initial cost, limiting their wider use in marine industries [18]. Furthermore, marine structures experience various loads during their operational lifespan [19]. These loads can be broadly classified into static, dynamic, and repeated loads. Static loads include the weight distribution per unit area of the structure, combining shear and bending stress [20]. Examples of static loads include: (i) wave-bending-moment, (ii) horizontal-bending-moment, (iii) torsional-moment, (iv) external-hydrostatic load, and (v) internal load. Dynamic external loads are generated by waves and cause torsional bending moment and raking stress [21, 22]. The dynamic load can lead to cyclic loading and fatigue. The interaction of waves with a ship structure causes acceleration, leading to vibration loading [23, 24]. To counteract racking stresses caused by pitching and heaving, the front and back structures of a ship are reinforced with stringers, beams, and breast hooks [25]. Impact loading, known as slamming, occurs when water contacts the lower side of the front structure, inducing high shear force and bending moment from vertical waves [26]. Springing oscillation occurs when the wave's action repeats at a certain frequency, leading to cyclic loading and fatigue [27]. Miscellaneous loading, involving: (i) hydrodynamic, (ii) wind, sloshing, (iii) operational, and (iv) ship-handling loads, which are subjecting various components of marine structures to periodic stress [28, 29]. Therefore, Dynamic Mechanical Analysis (DMA) is commonly used to evaluate the performance of composite properties under changing temperature, time, and frequency conditions [30]. Specifically, DMA is used to analyze the viscoelastic properties of synthesized samples by varying temperature, time, and stress–strain loads. Key DMA test parameters include: (i) storage modulus, (ii) loss modulus, and (iii) DF, all of which are functions of temperature, time, and frequency [31].

In the previous years, numerous articles focused on DMA of hybrid fibers reinforced nanocomposites (many studies have been found on DMA with only one type of nanocomposites) [32–39]. For instance, Baral et al. [40] improved marine-sandwich-panels by reinforcing thickness and simulating slamming loading on sandwich-boat-structures with a weighted elastomer ball. They used Nomex honeycomb, foam, and pinned foam as cores with different densities and dimensions. The honeycomb-structures were made with high-strength CF R367-2 at two layers with ±45° and bonded with adhesive film ST 1035. The cure cycle was at temperature 100 °C for 4 h. and 0.9 bar vacuum. They found that the honeycomb-core-sandwich-panels are suitable for racing yacht hulls and could withstand impact energy up to 1200 J without damage, but they did not reach the highest expected value. Therefore, another related study attempted to enhance the performance of composite sandwich panels by Redmann et al. [32]. Redmann et al. [32] conducted high force DMA tests for non-destructive evaluation of composite sandwich panels. They used various materials, including CF, aluminium alloy 5056, and aramid Nomex for the panels, with different core materials such as aluminium core with 0.25-inch and 0.50-inch, and aramid core with 0.25-inch. Vacuum moulding technique was employed to construct the panels, and they underwent post-cure at temperatures of 90 °C for aluminium-core-panels and 65 °C for aramid-cure-temperatures. Different frequencies from 1 to 100 Kz were applied to evaluate the optimum stiffness and damping ability of the cores. The study concluded that the stiffness of composites-sandwich-panels was influenced by two factors: static load and the type of core material. Additionally, the glass transition temperatures (Tg) of the peak in the loss modulus (E″) were found to be 154 °C for aluminium core with 0.25-inch and 119 °C for aramid core with 0.25-inch, indicating a moderate Tg value. Therefore, another article focused on improving vibration and damping properties through adding one kind of nano-powders by Alsaadi et al. [33]. They investigated the influence of incorporating nano-silica on the static tests (tensile and flexural) and dynamic tests, such as DMA, of hybrid woven CF and Kevlar reinforced with polymers. The reinforcement comprised woven CF/Kevlar with a density of 190 g/m$^3$, while the matrix was epoxy resin MGS L285, and the nanoparticles were nano-silica with a diameter of 1–10 nm. Different weight fractions of nano-silica (0.5, 1, 1.5, 2.5, and 3 wt.%) were added to eight

layers of CF/Kevlar using the hand lay-up technique. The samples were cured at 80 °C temperature, 120 kPa pressure, and 1 h time. The addition of 3 wt.% nano-silica resulted in a 20% improvement in tensile strength and a 35.7% improvement in flexural strength compared to the unmodified sample. The study also highlighted the beneficial interaction between nano-silica, epoxy, and fibers (CF/Kevlar), which enhanced the vibration and damping properties, but they did not reach the highest expected value, this is due to: (i) not using an innovative dispersion method, (ii) not applying a vacuum technique, and (iii) not adding dual nano-powders. Similar article was concerned on improving damping properties of hybrid CGF reinforced with epoxy by Muralidhara et al. [34]. They studied the effect of addition graphene nanoplatelets (GNPs) (0.75%, 1.75%, and 2.75 wt.%) on morphological, tensile, and DMA of hybrid CGF reinforced with epoxy. They used woven CGF as reinforcement while Araldite LY1564 as matrix and GNPs as nanofillers. They used process of mixing through ultra-sonication at 20 kHz at 5 s of pulse rate to disperse GNPs inside matrix. They used the method of vacuum bagging to fabricate the samples. They concluded that the addition of GNPs at 1.75%, and 2.75 wt.% was improved tensile strength compared to GNPs at 0.75wt.%. They also elucidated that the addition of GNPs at 1.75 wt.% was improved damping properties.

According to the pervious literature review, it can be noted that there are few studies focused on studying the effect of adding dual fillers of nano-powders on DMA of hybrid CGF for purposes of naval structures. Accordingly, this article focused on three specific research questions or hypotheses as follows: (i) Can hybrid composite structures be successfully synthesized by adding nanoparticles ($Al_2O_3$ + GNPs) using a simple and cost-effective method?; (ii) How does the incorporation of nanoparticles ($Al_2O_3$ + GNPs) into hybrid woven CGF affect the morphological and microstructural characteristics of the composite material before and after DMA? And (iii) What is the impact of adding dual fillers of GNPs and $Al_2O_3$ on the damping properties (complex viscosity, storage modulus, loss modulus, dynamic capacity, and glass transition temperature) of hybrid CGF reinforced for marine structures? Therefore, the main objective of this study is divided into three specific goals. The first objective is to synthesis hybrid composite structures with adding nanoparticles ($Al_2O_3$ + GNPs) with simple and cheap route. The second objective of this

study is to investigate the influence of nanoparticles additives incorporation on the morphological, and microstructural characteristics of hybrid woven CGF before and after DMA. The third objective of this study is to investigate the role of adding dual fillers of GNPs and $Al_2O_3$ on improving the damping properties: ((i) complex viscosity, (ii) storage modulus, (iii) loss modulus, (iv) dynamic capacity, and (v) glass transition temperature (Tg)) of hybrid CGF reinforced for purposes of marine structures.

In this work, multi-scale hybridization between CF, GF and nano-powders in composite materials has been investigated; this domain is a new research area. Thus, there are main contributions in this work is to: (i) using two dual different additives of nano-powders, applying new dispersion method, and using hybrid of different woven fabrics fibers in order to fabricate unique marine structures. For the first time, this study focuses on scattering dual nano-powders in hybrid CGF reinforced polymer for reinforcing the weak portion of the composite materials used in manufacturing of marine structures. This study presents novel and simple procedures to fabricate the nanoparticles of hybrid CGF with different contents of GNPs and $Al_2O_3$ for marine structures applications. This study focuses on evaluating developed composites based on different measures and analyses such as microstructural, morphological, and DMA to simulate different applied loads in marine structures.

After exploring literature review about importance of produce marine structures with dual contents of nano-powders inside hybrid CGF reinforced epoxy to enhance damping characteristics, it can be explored experimental details in Sect. 2.

## 2 Experimental Work

In this study, we will illustrate the details about experimental work (materials, preparation techniques, and tests). In order to prepare the composite specimens epoxy (Sikadur 330) is used as a matrix and GF and/or CF was used as reinforcement materials. Furthermore, aluminium oxide $Al_2O_3$ and/or graphene nanoplatelets (GNPs) were used as nano-additives to strengthen the prepared composites. The mechanical properties of the main constituent of the prepared composites are tabulated in Table 1. Both of GF and CF have a fabric form which composed of two perpendicularly interlaced sets of

**Table 1** Mechanical properties of the main constituent of the prepared composites [6]

| Properties | Epoxy | Carbon fiber | E-glass fiber | GNPs | $Al_2O_3$ |
|---|---|---|---|---|---|
| Tensile strength (MPa) | 30 | 2400 | 1400 | 167 | 665 |
| Poisson's ratio | 0.35 | 0.30 | 0.22 | 0.012 | 0.24 |
| Tensile modulus (GPa) | 4.1 | 228 | 72.3 | $2.4 \times 10^3$ | 210 |
| Density (g/cm$^3$) | 1.16 | 1.6 | 2.56 | 2.267 | 3.78 |

fiber yarns. The first set of those yarns is called the longitudinal or warp yarns and the second set is called transverse or fill yarns. The used $Al_2O_3$ nanoparticles were white in colour and spherical in shape with a density of 3.78 gm/cm$^3$, an average diameter less than 25 nm, and purity of ~95%. GNPs were grey in colour and flake in shape with a density of 2.267 gm/cm$^3$, and an average size less than 100 nm. One of the most important factors determining the properties of composites is the relative proportion of the matrix and reinforcing material. The relative proportions can be given as weight fractions or volume fractions. The weight fraction is easier to be controlled during fabrication, or to be determined experimentally after composite fabrication. These expressions are usually derived for two–phase materials, and then generalized to a multi-phase material. The theoretical value of fiber volume fraction is estimated from the weight of fiber and resin for a required plate dimension. The volume fraction of fibers ($v_f$) was experimentally measured using burning technique based on ASTMD-3171-99 [35]. ASTM D 3171-99 can be extended to characterize carbon/glass hybrids [36]. Accordingly, a constant volume fraction of 32% was determined for specimens. Five layered structures were prepared, namely glass fiber-reinforced epoxy, carbon fiber-reinforced epoxy, hybrid glass/carbon fiber-reinforced epoxy, and hybrid glass/carbon fiber-reinforced epoxy with 1.5 wt. % and 3 wt. % of GNPs/$Al_2O_3$ nanoparticles. The prepared composites are mentioned in Table 2.

The preparation process of different composite structures is executed based on the procedures described in ref. [6]. Nanoparticles are treated using a non-reactive modifier (stearic acid + ethyl-acetate solution) to increase its adhesion with epoxy. A mechanical mixer is used to mix stearic acid with ethyl-acetate solution for ½ hour and to mix the produced solution with nanoparticles for another ½ hour as shown in Fig. 1. Then, the nanoparticles are washed using ethyl-acetate solution to remove stearic acid. To ensure dispersion homogeneity of the nanoparticles into the epoxy matrix, the material blend is subjected to ultra-sonication process. Henan Lanphan (UP200S) mechanical stirrer was used at 500 RPM for 30 min to achieve uniform dispersion of the nano-additives. During sonication process, the applied frequency was 0.5 cycles per second

and the amplitude was 70% of the device amplitude. The sonication time was 3 h to avert the nanoparticles agglomeration. To avert the degradation of epoxy, the nanoparticles/epoxy blend was cooled down in an ice bath prior to sonication process. Then, the hardener was added to the epoxy resin with a weight ratio of 1:2. Finally, the blend is going through a curing process for 30 min at a temperature of 55 °C. The hand lay-up technique has been used to fabricate the composite structures. The composite structures are fabricated layer by layer until the desired number of layers is achieved. Then, the compression mold method is used to obtain the final composite with dimensions of $200 \times 300$ mm. After the curing process, test samples are cut from the produced composite to match the standard dimensions of each test. After the fabrication process, the produced samples are evaluated based on morphological and microstructural tests such as optical microscopy (OM), scanning electron microscopy (SEM), and energy-dispersive X-ray spectroscopy (EDS) before and after DMA testing. The microstructural specimens were prepared through mounting, then mechanical grinding, and polishing according to the standard metallography practices. DMA tests were carried out three-point bending test with dual cantilever through machine tester of DMA with setup DMA/SDTA861$^e$, in order to evaluate viscoelastic characteristics of synthesized samples to suitable the purposes of marine applications. The test specimens were prepared with dimensions of 50 mm $\times$ 10 mm $\times$ 2.3 mm, following the ASTM D4065 standard. Before beginning DMA test, all test specimens were kept isothermal temperature at 5 min during 1 Hz, in order to obtain thermal stability. The characteristics of viscoelastic were obtained through changing different values of heating temperatures from 10 to 105 °C and several magnitudes of dwelling time from 5 to 575 min at 1 Hz frequency with heating rate at 4 °C/min at 20 ml/min of nitrogen flow rate. A computer-based data acquisition system was used to controlled machine operation and data recording. A total of 36 specimens were tested in this study, with 3 samples evaluated for each case, and the average values were calculated. This type of test provides valuable information about the integrity of the tested sample by analyzing the energy absorbed during the

**Table 2** Prepared specimens in the present study

| No | Name specimens | Weight percentage of nanoparticles |
|---|---|---|
| S1 | Glass fiber-reinforced epoxy (GF) | None |
| S2 | Carbon fiber-reinforced epoxy (CF) | None |
| S3 | Hybrid carbon/glass fiber-reinforced epoxy (CGF) | None |
| S4 | Hybrid carbon/glass fiber-reinforced epoxy with GNPs/$Al_2O_3$ nanoparticles (CGF-1.5% wt. GA) | 1.5% wt. $Al_2O_3$ + 1.5% wt. GNPs |
| S5 | Hybrid carbon/glass fiber-reinforced epoxy with $Al_2O_3$ nanoparticles (CGF- 3% wt. GA) | 3%wt. $Al_2O_3$ + 3%wt. GNPs |

**Fig. 1** Fabrication process of the hybrid carbon/glass fibers reinforced by GNPs and Al$_2$O$_3$
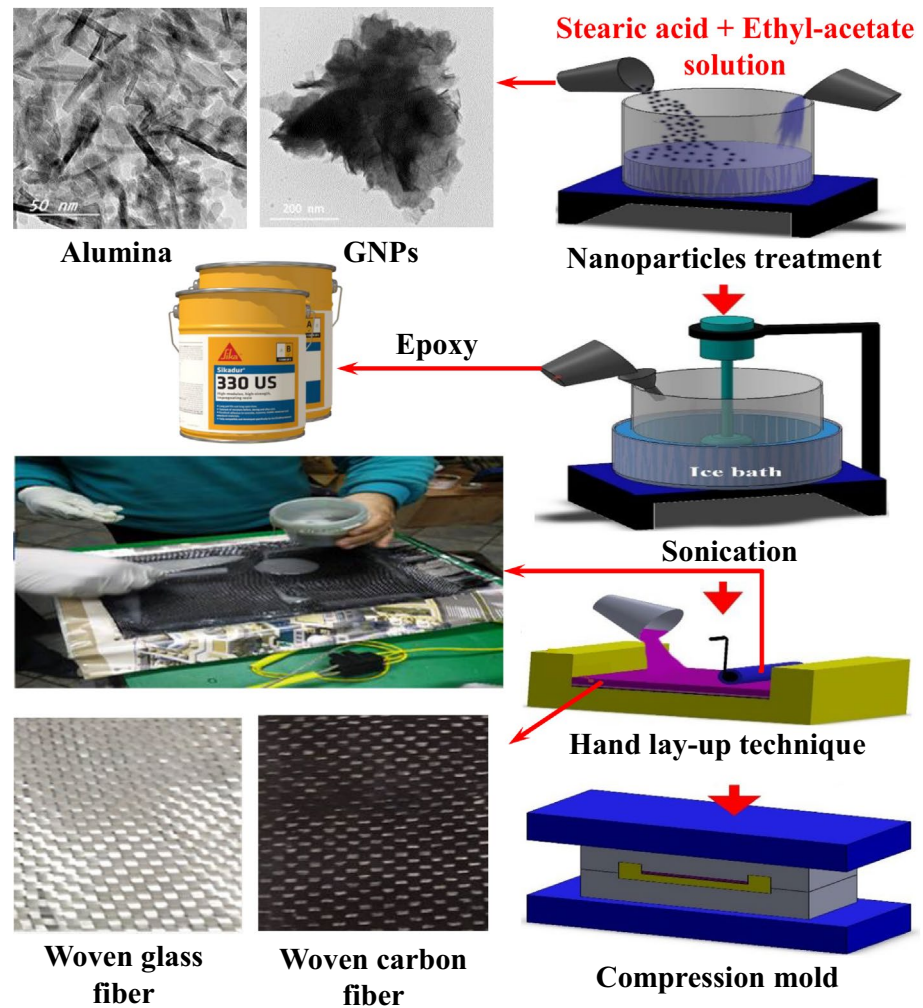


test, which is then compared to the results obtained from reinforced and unreinforced specimens.

## 3 Results and Discussion

### 3.1 Microstructure Characterization of Synthesized Specimens Before DMA

The use of Al$_2$O$_3$ and GNPs as nano-additives will be discussed in this section considering the microstructure characterization of the produced composites before the DMTA.

The optical microscope images of the microstructure for different prepared specimens are shown in Fig. 2. Many bubbles are observed in the specimen surface in case of GF as shown in Fig. 2a due to the large distance between the used GF, the high amount of resin, and the insufficient applied pressure during the hot press process. These reasons result in formation of bubbles, which create voids and pores between the fibers. Many reasons cause the formation of bubbles such as the differences between interactions, dimensions, densities, and volume fractions of the two woven fibers. Additionally, the differences between physical and chemical properties such as concentration, and orientation as well as dispersion method, treatment state and manufacturing method may cause in bubbles formation. This result can weaken properties of synthesized samples [6]. In the second case (CF) shown Fig. 2b, it can be observed that there is no pores on the woven surface of CF which reveals the use of the correct distance between the CF as well as the sufficient amount of epoxy which activate the capillary effect generating an impregnation on the surface of the homogeneous fiber. This observed can improve the mechanical characteristics of prepared specimens [8]. In case of CGF shown Fig. 2c, voids and bubbles are observed between the carbon and Gf as the volume fractions and dimensions of carbon and GF are different. The existence of these bubbles could be diminished by adding nanoparticles, as they are filling these undesirable vacancies. This observed can enhance the characteristics of prepared specimens [6]. In case CGF-1.5% wt. GA shown Fig. 2d, it is observed that there are no voids or bubbles on the produced surface thanks

**Fig. 2** Optical microscope images of the fabricated composites: **a** GF, **b** CF, **c** CGF, **d** CGF-1.5% wt. GA and e CGF-3% wt. GA
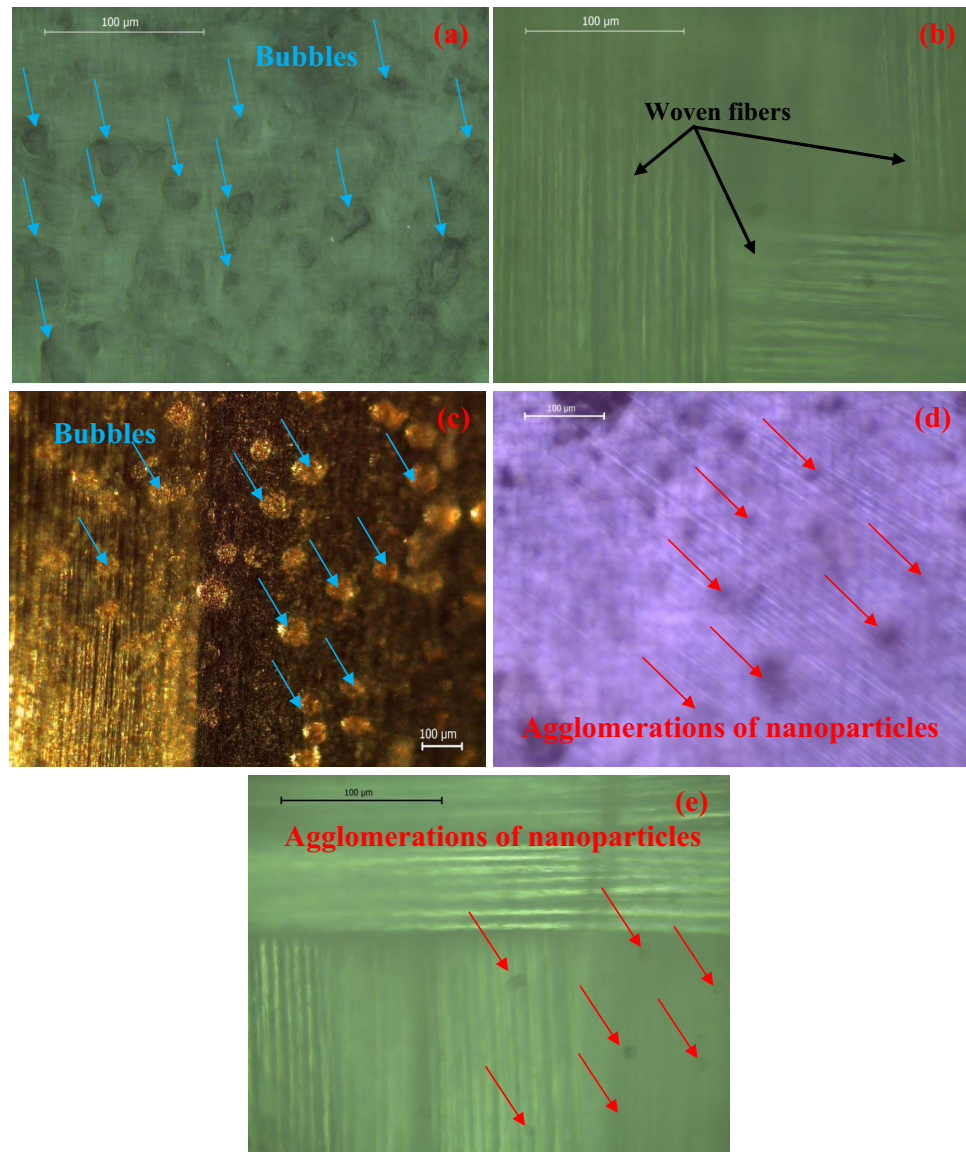


to the nanoparticles which are uniformly scattered and fill the vacancies on the produced surface. This observed makes the mechanical properties of prepared samples unique [6]. In case CGF-3% wt. GA shown Fig. 2e, it is observed that $Al_2O_3$ nanoparticles are agglomerated between CF and GF, which help in preventing undesirable voids and bubbles. The observed phenomenon results in poor mechanical characteristics of the prepared samples [8]. Figure 3 elucidates the SEM images of the prepared samples. It could be observed that bonding occurs between the GF and epoxy for the GF sample, which causes remarkable porosity and pore volume. The formed pores are significantly decreased in CF samples.

CGF sample have acceptable surface compared with GF surface. CGF-1.5% wt. GA sample has a uniform scattering of nanoparticles, which helps in transmitting the stress from the epoxy to the carbon and glass fibers. Finally, a very good

scattering of $Al_2O_3$ nanoparticles is observed on the surface of CGF-3% wt. GA samples thanks to the high frequency sonication process used in producing nanoparticles/epoxy mixture, this discovery in this study is consistent with the outcomes reported by Abu-Okail [6, 8].

Figure 4 shows the SEM images perpendicular to the fibers of the fabricated samples. More nanopores are detected between the fibers of GF samples compared with that of CF samples. Nanobubbles are detected in CGF samples due to the variation in dimensions and density between carbon and GF. Uniform scattering of $Al_2O_3$ and GNPs was detected in CGF-1.5% wt. GA samples. This uniform scattering enhances the properties of the fabricated samples which reduces the agglomeration of the nanoparticles, strengthens the bonding of the composite components, and transmits stress concentration

**Fig. 3** SEM images parallel to the fibers of the fabricated composites: **a** GF, **b** CF, **c** CGF, **d** CGF-1.5% wt. GA and **e** CGF-3% wt. GA
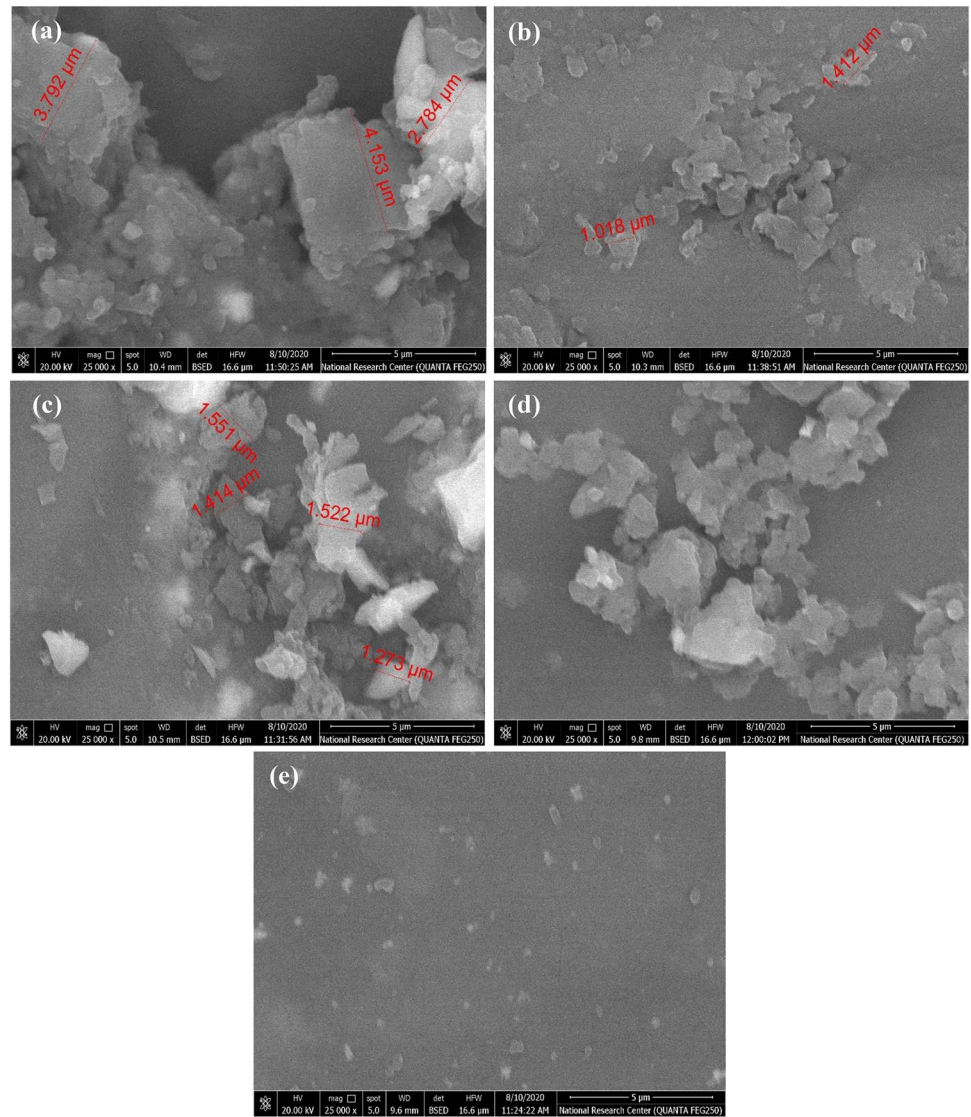


from epoxy to enhance the mechanical properties of the fabricated samples [34]. It could be observed that bonding occurs between the GF and epoxy for the GF sample, which causes remarkable porosity and pore volume (this is elucidated clearly in Fig. 4a). Finally, $Al_2O_3$ nanoparticles are agglomerated in CGF-3% wt. GA samples, which impair the bonding between the epoxy and fiber.

Figure 5 shows map analysis and FE-SEM image of CGF-1.5% wt. GA sample. The FE-SEM images show a uniform scattering of the nanoparticles on the surface of the sample thanks to the well-performed sonication process. The EDS analysis reveals that the weight fraction of Al, O and C elements is 0.42%, 23.68% and 75.9%, respectively. The highest weight fraction was observed for C element as carbon is the main element of graphene as well as carbon and GF. Oxygen element is detected in alumina as well as the formed bubbles, this outcome aligns with Abu-Okail et al. [6].

## 3.2 DMTA of Synthesized Specimens

DMTA is a basic experimental technique used for measuring the viscoelastic behaviour of polymers and their composites. A sinusoidal force (stress $\sigma$) is applied to a polymeric sample and its corresponding displacement (strain) is simultaneously measured. The temperature or frequency can also be varied during the test and the DMTA parameters are measured simultaneously. The typical DMTA parameters of interest for composite polymers are storage modulus (E′), loss modulus (E″), damping factor (DF) or loss factor (tan δ), and complex viscosity ($\eta^*$) as a function of temperature, time or frequency [37]. These parameters are usually connected to the molecular movements and phase transition processes. The E′ measures the stored energy and reflects the material's stiffness and elastic behaviour meanwhile E″ explains the material's viscous

**Fig. 4** SEM images perpendicular to the fibers of the fabricated composites: **a** GF, **b** CF, **c** CGF, **d** CGF-1.5% wt. GA and **e** CGF-3% wt. GA
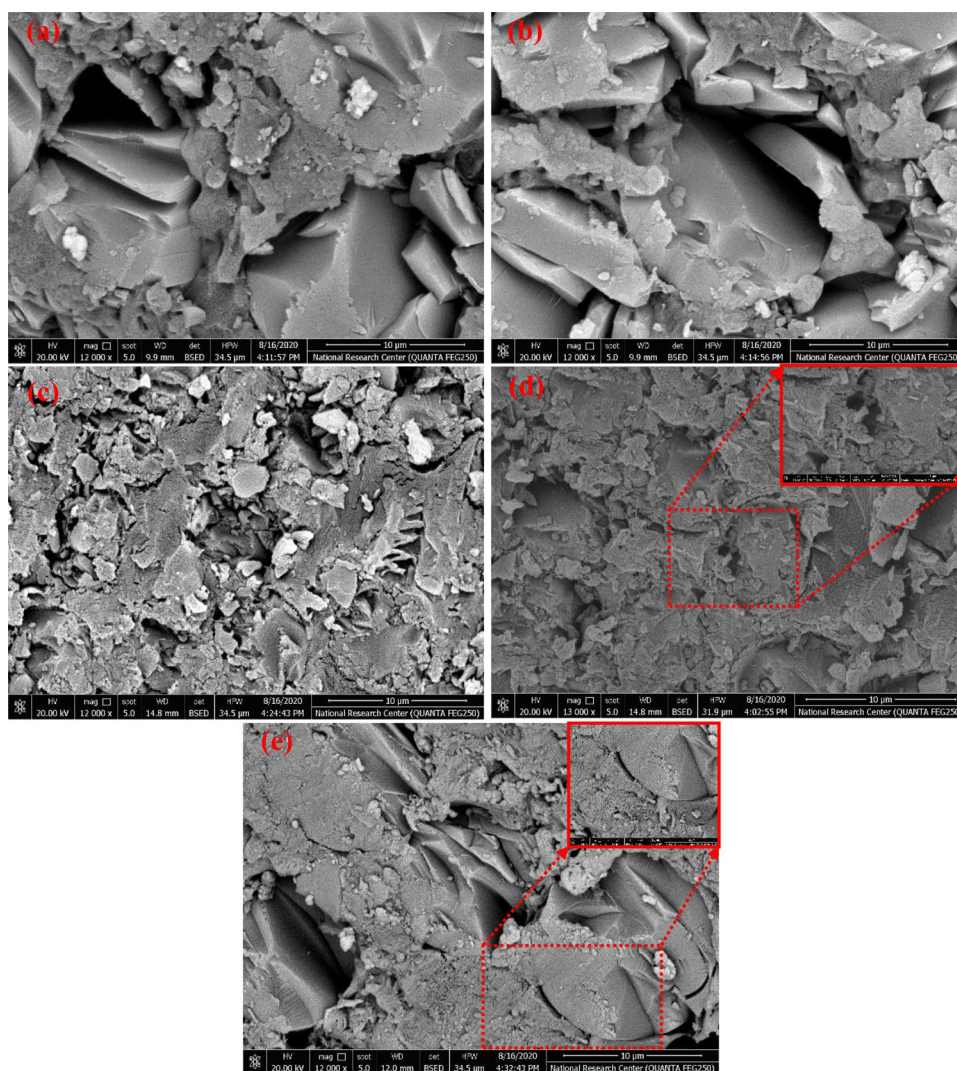


response and it is associated with the energy dissipation [18]. The complex modulus ($E^*$) describes the material's elasticity and it is the sum of $E'$ and $E''$ as illustrated in Eq. 1. The $D^*$ is the reciprocal value of the $E^*$ ($D^* = 1/E^*$) and used for measuring polymers softness. The measuring units for $E'$, $E''$ and $E^*$ are megapascals (MPa), which are units of stress.

$$E^*(\omega) = E'(\omega) + iE''(\omega). \tag{1}$$

The damping factor or loss factor (DF) results from dividing the $E''$ on $E'$ (Eq. 2) and indicates the material's elasticity and rigidity. DF improves the safety of a structure by absorbing energy from impacts. It is a dimensionless quantity that represents the amount of energy dissipation or damping in polymeric materials. For instance, a DF of 0.07 indicates that 7% of the energy is dissipated or lost for each cycle of deformation or oscillation. Similarly, a DF of 0.3 represents 30% energy dissipation per cycle.

$$\tan\delta = \frac{E''}{E'}. \tag{2}$$

The $\eta^*$ measures the total resistance to flow of polymers under the influence of an applied stress or shear rate. It was studied with temperature to provide information about polymers processability. Complex viscosity is measured in pascal-seconds (Pa·s).

DMTA is also used for measuring the glass transition temperature ($T_g$) of amorphous polymers. The $T_g$ is a temperature at which a polymeric material is changed from a rigid structure to a rubbery state. The $T_g$ is the corresponding temperature to the maximum peak of the DF (tan δ). The $T_g$ is depending mainly on the crosslink density and the degree of branching of the polymeric materials [38]. For instance, thermosets have high crosslink density and that results in higher $T_g$, higher modulus and low DF due to the molecular motion restriction [39]. Contrary, thermoplastics have lower $T_g$

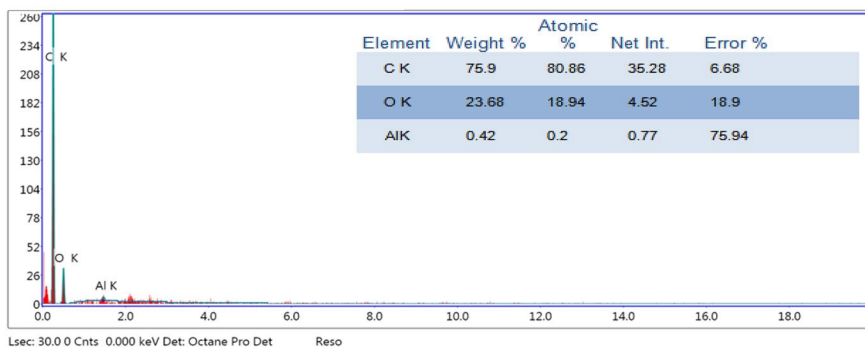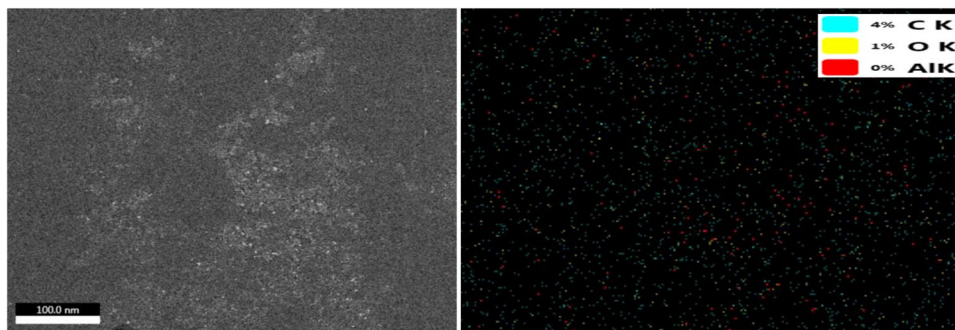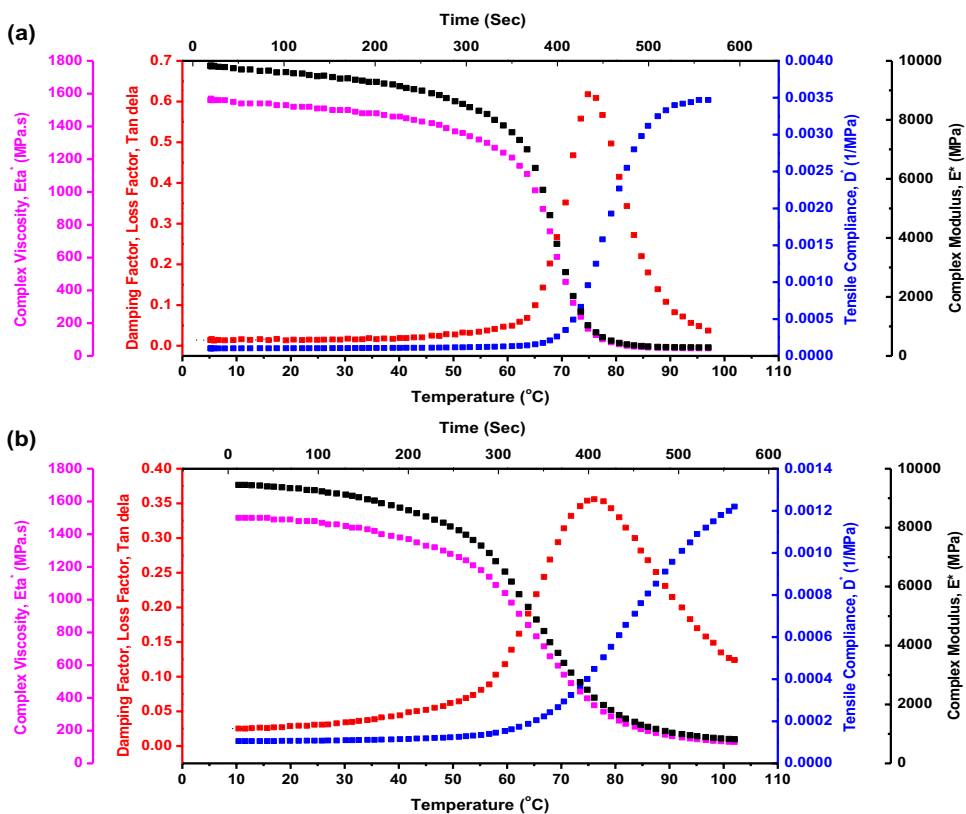**Fig. 5** FE-SEM image and map of CGF-1.5% wt. GA sample



**Fig. 6** DMTA of **a** CF **b** GF



values, lower modulus and high DF due to its lighter crosslinking [41].

Figure 6a, b presents the DMTA parameters of CF and GF with temperature and time. The presented values are the average of three highly precise and consistent measurements, with a maximum error of less than 1%. Generally, the E* and η* values were decreased with the temperature increase for both the CF and GF. Contrary, D* was

increased with temperature increase. It was also noticed that all the DMTA parameters for the CF are changed drastically with temperature and time if it compared with the GF which changes gradually. As it can be seen from Fig. 6a, the values of the DF for the fabricated CF are almost stable at low temperatures, while after about the 60 °C, a sharp increase can be observed until a peak value, then a sharp decrease is obtained until low values. On the other hand, Fig. 6b shows a gradual increase in the DF with temperature increase until reaching to the peak value and then gradually decreases until reaching to lower values (broad curve). Usually, this steep fall determines the maximum operating temperature of the polymeric materials. The DMTA results of E, D, $\eta^*$ and DF for both CF and GF are consistent with the previously presented microstructure shown in Figs. 2, 3, and 4.

The highest detectable value of the DF for the CF and GF are 0.62 and 0.36 at 74.8 °C and 76.1 °C, respectively. Obviously, the highest DF for both the CF and GF are located at the same $T_g$ nearly. However, it is higher in case of CF by about 0.26, This is because CF have a more disordered structure than GF, which allows them to dissipate more energy as heat, which indicates that the CF is more elastic than the GF as it can easily deform without failure when subjected to external force [42]. Generally, CF has a higher DF than GF [43].

Figure 7a, b, c presents the DMTA of the hybrid CGF, hybrid CGF-1.5% wt. GA and hybrid CGF-3% wt. GA, respectively. It was noticed that the DF for the hybrid CGF, hybrid CGF-1.5% wt. GA and hybrid CGF-3% wt. GA are 0.65, 0.68 and 0.54 at $T_g$ 35 °C, 73.4 °C, and 27.8 °C, respectively. The DF curve shown in Fig. 7a is changing



**Fig. 7** DMTA of the hybrid **a** CGF, **b** CGF-1.5% wt. GA, **c** CGF-3% wt. GA
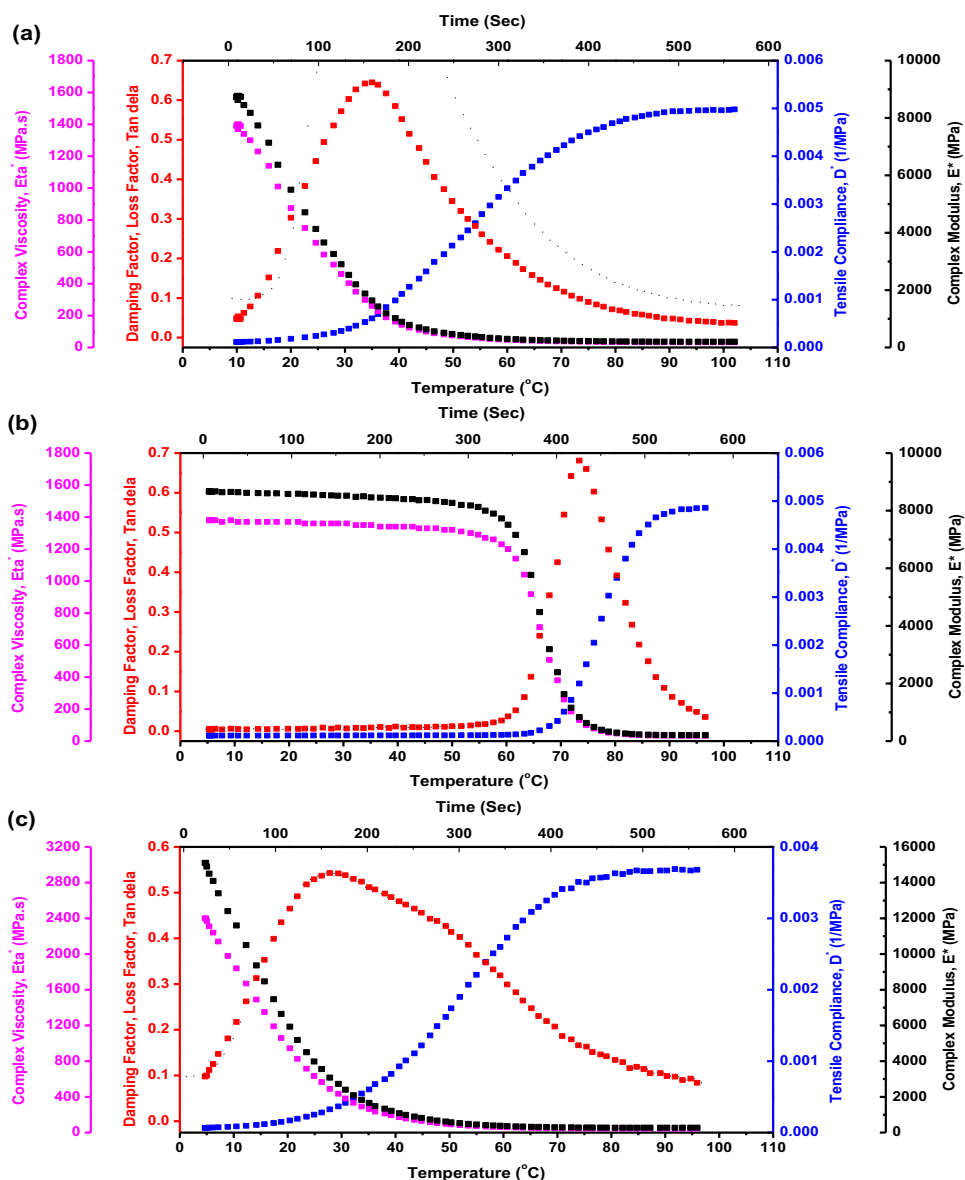
gradually, while that of Fig. 7b is sharply changed. Furthermore, Fig. 7c shows the lowest change for the DF with temperature.

Figure 8a, b presents a clear comparison between the DF of CF, GF, CGF, CGF-1.5% wt. GA and CGF-3% wt. GA with the temperature and time variation. The measured results shown in Fig. 8a were fitted using a Lorentzian curve. It was noticed that the temperature and time have the same effect on the DF variation due to the linear relationship between time and temperature. The values of $T_g$ and maximum DF of all the prepared fibers are investigated from the figure and tabulated in Table 3. In addition, Table 3 provides a clear comparison of our investigated results to other references [44–47]. The resulting graph of the prepared CGF composite has merged the maximum DF of the CF and the broad shape of the GF curve. In addition, the $T_g$ value was shifted toward the lower temperature (35 °C) and the change from the glassy state to rubbery state was occurred at 164 s instead of 435 s and 407 s for CF and GF, respectively. The higher DF of the CGF is attributed to greater interfacial bonding between the fibers and matrix components.

However, the low $T_g$ value is attributed to the presence of different voids and bubbles between the hybrid carbon and GF as shown in Fig. 2c. This is due to the differences between dimensions, interactions, and volume fractions of the carbon and GF [6]. The addition of the nanomaterials (Graphene & $Al_2O_3$) to the CGF by about 1.5% enhanced the DF to higher value (0.68) as indicated in Table 3. Furthermore, the $T_g$ was also increased to 73.4 °C. The higher values of the DF and $T_g$ of the hybrid CGF-1.5% wt. GA are due to the voids and bubbles disappearing as the nanoparticles are uniformly scattered and fill the vacancies on the produced surface as shown in Fig. 2d. Increasing the amount of nanoparticles in the hybrid CGF-3% wt. GA leads to deteriorate the DF and $T_g$ as they reduce the bonding between the CF and GF. The results of this study were compared to those of natural fiber-reinforced polymers. For example, the results of Merzoug et al. [44] on DF and Tg are comparable to our measurements for Hybrid CGF + 1.5% GNPs + 1.5% $Al_2O_3$. However, the DF results measured by Atiqah et al. [45] are lower than all of our measurements for all prepared materials, as shown in Table 3. Additionally, the measured
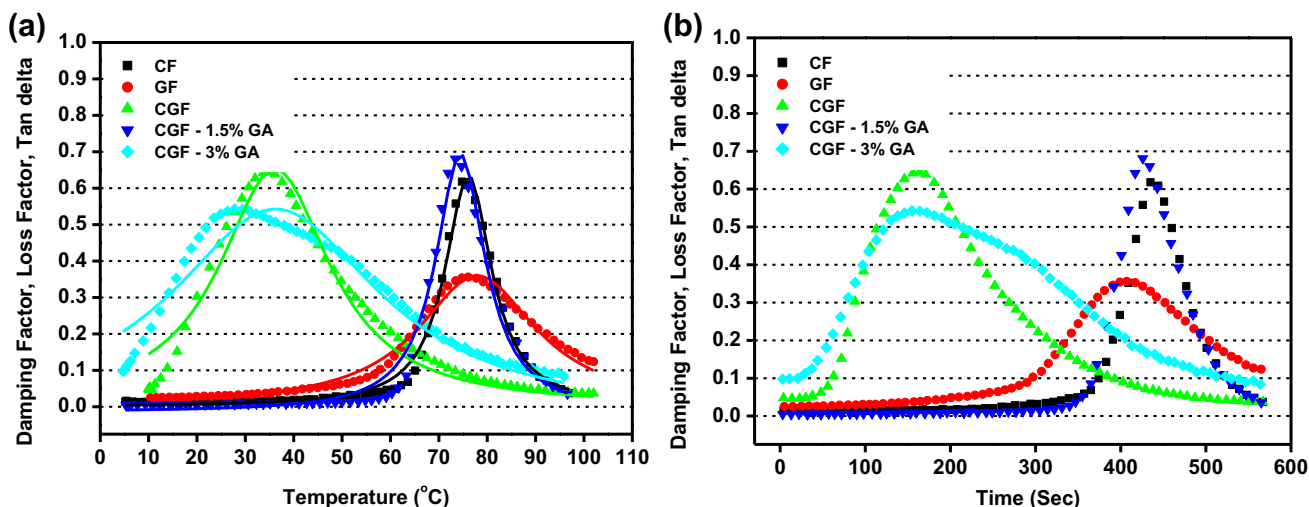


Fig. 8 DF of the hybrid carbon/glass fibers with **a** temperature **b** time

Table 3 $T_g$ and maximum DF of the prepared fibers

| No | Specimen name | Matrix | $T_g$ (°C) | DF | References |
|----|---------------|--------|------------|-----|------------|
| 1 | CF | Epoxy | 74.8 | 0.62 | This work |
| 2 | GF | | 76.1 | 0.36 | |
| 3 | Hybrid CGF | | 35 | 0.65 | |
| 4 | Hybrid CGF + 1.5% GNPs + 1.5% $Al_2O_3$ | | 73.4 | 0.68 | |
| 5 | Hybrid CGF + 3% GNPs + 3% $Al_2O_3$ | | 27.8 | 0.54 | |
| 6 | Hybrid Sugar palm/Glass fiber | Polyurethane | −10.52 | 0.23 | [45] |
| 7 | Hybrid Date palm petiole/Glass | Vinyl ester | 75.3 | 0.66 | [44] |
| 8 | GNPs (S5G0) | Epoxy | 67.77 | 0.46 | [46] |
| 9 | rGO 1% | Epoxy | 144 | 0.29 | [47] |

data were compared to carbon-based nanocomposites such as multiwall carbon nanotubes (MWCNTs) and reduced graphene oxide (rGO). Jesuarockiam et al. [46] reported a DF of 46 for GNPs/Epoxy at a Tg of 67.77 °C. Kamble et al. [47] reported a DF of 29 for rGO 1%/Epoxy at a Tg of 144 °C. Table 4 provides a statistical comparison of the measured DF for all prepared samples to their Lorentz fit, with a maximum error of 1%. A lower error indicates that the measured data is less noisy and more accurate. This is because the noise in the data will cause the measured values to deviate from the actual values, and the lower the noise, the smaller the deviation will be.

Figure 9 presents the E* with temperature and time for all the prepared samples. The change of the E* values with temperature and time for CF, GF and CGF-1.5% wt. GA follows the accepted trend. However, the CGF and CGF-3%

wt. GA show lower E* values. For CGF, the lower values are attributed to the presence of voids and bubbles between the hybrid carbon and GF, as shown in Fig. 2c. These voids and bubbles are formed due to the differences between the dimensions, interactions, and volume fractions of the CF and GF. For the CGF-3% wt. GA, the lower values are due to the nanoparticles agglomeration, which reduces the bonding between the CF and GF within the epoxy matrix as shown in Fig. 2e. Alarifi reported in his study that the E* of GF is higher than CF at elevated temperatures [48].

On the other hand, Fig. 10 provides the same results presented in Fig. 9 but from the point of view of the compliance. It is clear that the compliance of the CGF and CGF-3% wt. GA started early if it is compared with the CF, GF and CGF-1.5% wt. GA. In addition, Fig. 11 also shows the same effect but from the point of view of the η*. The stiffness of

**Table 4** Data analysis for the DF of all the prepared materials

| Name of specimen | Measurements | Max | Mean | Standard division |
|---|---|---|---|---|
| GF | Measured values | 0.356 | 0.13821 | 0.11425 |
| | Lorentz fit | 0.35927 | 0.13758 | 0.11297 |
| | Absolute error (%) | 0.327 | 0.063 | 0.128 |
| CF | Measured values | 0.618 | 0.10969 | 0.1668 |
| | Lorentz fit | 0.62769 | 0.11202 | 0.16597 |
| | Absolute error (%) | 0.969 | 0.233 | 0.083 |
| CGF | Measured values | 0.645 | 0.23105 | 0.20569 |
| | Lorentz fit | 0.65257 | 0.23887 | 0.20215 |
| | Absolute error (%) | 0.757 | 0.782 | 0.354 |
| CGF-1.5% wt. GA | Measured values | 0.681 | 0.11875 | 0.1935 |
| | Lorentz fit | 0.68955 | 0.11808 | 0.18888 |
| | Absolute error (%) | 0.855 | 0.067 | 0.462 |
| CGF- 3% wt. GA | Measured values | 0.543 | 0.29822 | 0.16249 |
| | Lorentz fit | 0.54273 | 0.30397 | 0.15679 |
| | Absolute error (%) | 0.027 | 0.575 | 0.57 |
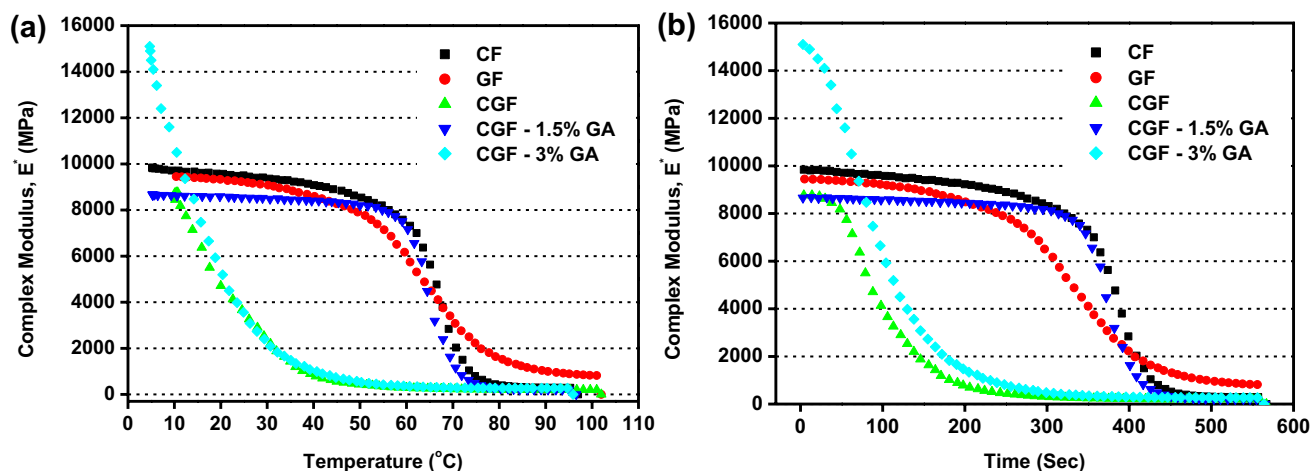


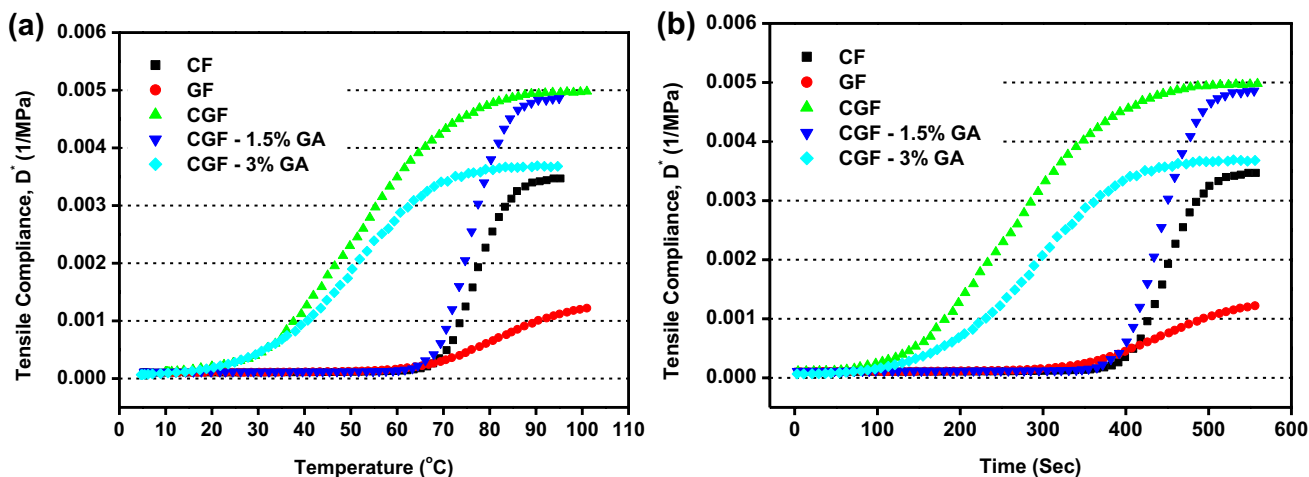**Fig. 9** Complex Modulus with **a** temperature **b** time

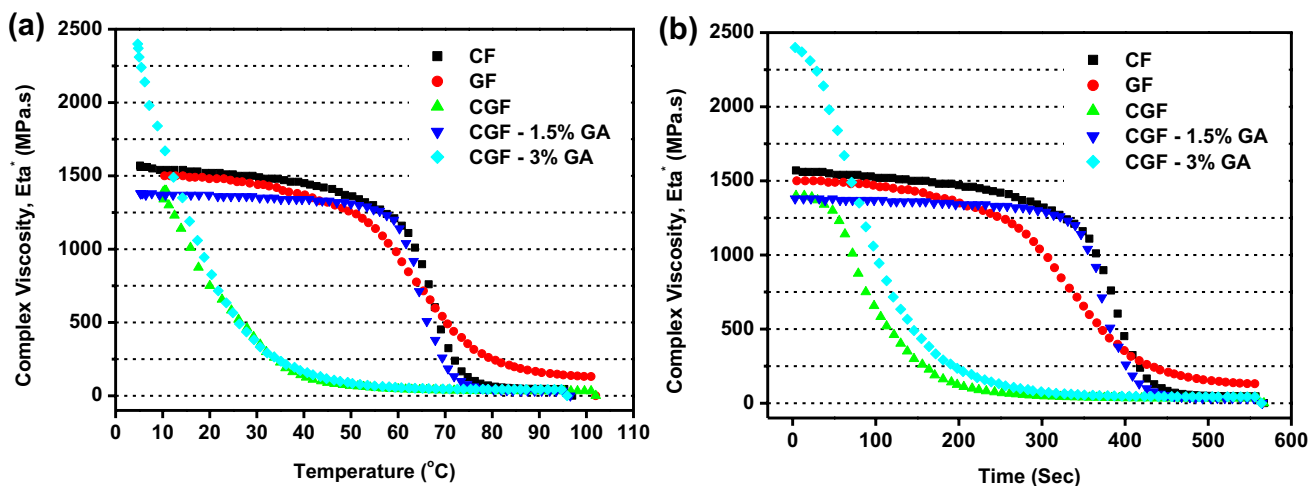**Fig. 10** Tensile compliance with **a** temperature **b** time



**Fig. 11** Complex viscosity with **a** temperature **b** time

### 3.3 Microstructure Characterization of Synthesized Specimens After DMA

After determining the major characteristics of dynamic mechanical: (i) storage modulus, (ii) loss modulus, (iii) damping factor, and (iv) glass transition temperature, it can be concern to fracture mode after DMTA tests. Therefore,

CF is higher than that of GF at temperatures below 65°C. Similarly, the stiffness of GF is higher than that of CGF-1.5% wt. GA at temperatures below 65°C. However, the trend is reversed above this temperature, meaning that GF becomes stiffer than CF and CF becomes stiffer than CGF-1.5% wt. GA. The measured properties are in line with the reported references [48–50]. In addition, the presented microstructures shown if Figs. 2, 3, and 4 are reflecting the measured values.

in this section, we will check failure mode of surfaces after tests of DMTA and compare between them. Figure 12 shows failed surfaces of CF in (a, b, c), GF in (d, e, f), and hybrid CGF-1.5% wt. GA in (g, h, i) with different magnifications through observing by SEM after DMTA tests. As we can see in Fig. 12a the magnification was 400x, it cannot be detected any cracks on the surface of CF, this is due to small magnification. Therefore, it can be taken deep magnification in Fig. 12b with 200x, the crack was detected in the surface of CF but the crack was small size (initiation crack stage), the crack length was about 0.125 μm. This is due to different factors: (i) the gap between fibers, (ii) moderate mechanical properties, and (iii) moderate adhesion between CF and matrix. In Fig. 12c shows the kind of fracture in the case of CF, the fracture mode in case of CF was brittle fracture. This finding in the present study corresponds with the results reported by Muralidhara et al. [34]. On the

**Fig. 12** SEM images for **a**, **b**, **c** CF, **d**, **e**, **f** GF, **g**, **h**, **i** Hybrid CGF-1.5% wt. GA
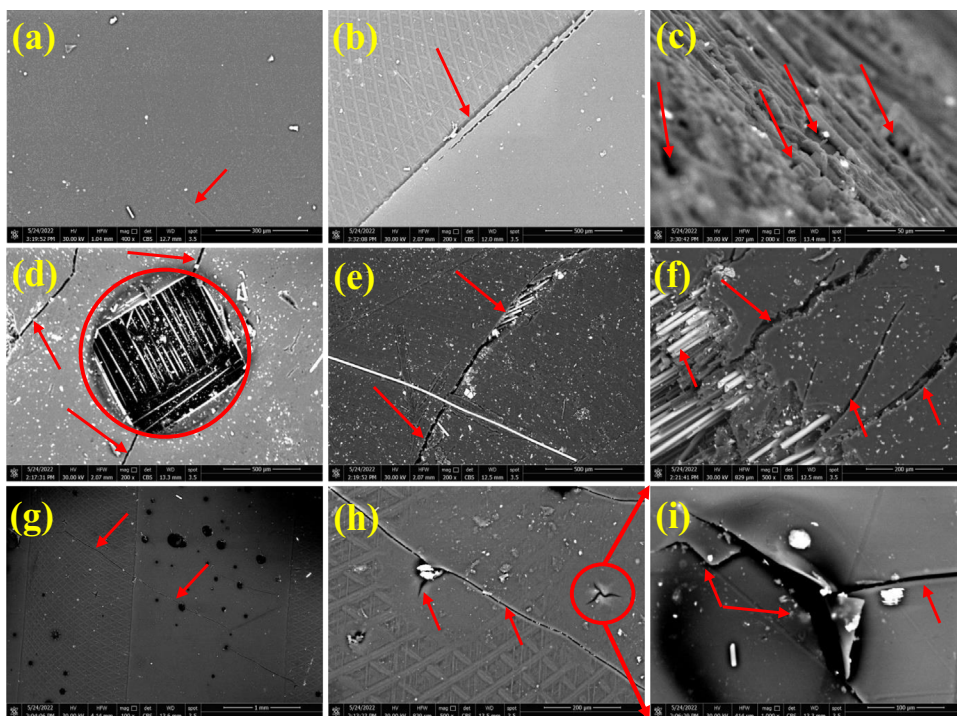


other hand, in Fig. 12d of GF, multi cracks were detected at 200 × magnification, this is due to the appearance of air bubbles, voids, and low adhesion between GF and matrix. This finding in the current study is consistent with the result of Ata et al. [5]. The crack length in Fig. 12d of GF was (0.25 μm) larger than in Fig. 12b of CF (0.125 μm). When comparing the crack size in the case of CF and GF, it can be found that the size of cracks in the GF (0.125 μm) are larger than in the CF (0.530 μm) see Fig. 12b and e, this finding in the current study is consistent with the result of Li et al. [35]. The cracks in the case of GF were propagated (propagation cracks stage). The type of failure in the case of GF was pullout, delamination, and cutoff fibers (damage mode), although the crack length was about 0.24 μm see Fig. 12f. This observation in the present study corresponds with the results reported by Abu-Okail et al. [2–5]. On the other side, in Fig. 12g of hybrid CGF-1.5% wt. GA with 100 × magnification, it can be detected the smallest size of crack (0.106 μm) at the largest surface area, see Fig. 12h. This is due to good adhesion between fibers, matrix, and nano-powders. This mechanism contributes to enhance fracture toughness of prepared samples. The kind of fracture in the case of hybrid CGF-1.5% wt. GA was brittle with high resistance to crack initiation, see Fig. 12i. An important point can be deduced that the fracture toughness of hybrid CGF-1.5% wt. GA was the highest, this is due to the resistance to propagate cracks were increased this is because adding nano-powders inside matrix epoxy between hybrid CGF. Hence, the significance of this finding lies in enhancing the use of marine structures in the face of varying challenges

associated with environmental forces, corrosion, and fatigue under fluctuating time and temperature conditions.

## 4 Conclusion

In this work, multi-scale hybridization between CF, GF and nano-powders (AL$_2$O$_3$ and GNPs) in composite materials has been investigated; in order to improve the performance of marine structures and to overcome the limitations of conventional materials, improve performance, and contribute to the development of more efficient and sustainable marine infrastructure. The conclusions drawn from the obtained results and observations in this work can be summarized as follows:

- The significant change in complex modulus values observed at high temperatures for CGF-1.5% wt. GA holds great importance for marine structures. It highlights the material's response and behaviour under elevated temperature conditions, providing valuable insights for assessing its performance and suitability in marine applications.
- The fabricated hybrid carbon/glass with 1.5% wt. GA nanoparticles showed higher values for the DF (0.68) and the Tg (73.4 °C). Higher DF values indicate improved energy dissipation and reduced structural vibrations. This can lead to enhanced structural integrity, reduced fatigue, and increased resistance to dynamic loading, thereby improving the overall performance and durability of

marine structures. A higher Tg implies improved thermal stability and increased resistance to dimensional changes and deformation over a wider temperature range. This can ensure the structural integrity and long-term performance of marine structures under diverse environmental conditions.

- The fracture type in the case of hybrid CGF-1.5% wt. GA was brittle with high resistance to crack initiation and propagation. This characteristic is desirable for marine structures as it indicates a higher level of structural robustness and reduced susceptibility to sudden failure or catastrophic events. The material can withstand the demanding operational conditions without compromising its structural integrity.

- Hybrid CGF composite with 1.5% wt. GA nanoparticles, displayed the highest fracture toughness, underscoring its importance for marine structures. This significant improvement in crack resistance not only enhances structural integrity but also promotes safety by reducing the likelihood of sudden failures.

- The significant change in complex modulus values observed at high temperatures for CGF-1.5% wt. GA holds great importance for marine structures. It highlights the material's response and behaviour under elevated temperature conditions, providing valuable insights for assessing its performance and suitability in marine applications.

These findings can assist marine structural applications to produce new structures with extraordinary and unique properties. The research offers practical significance for marine structures. It provides insights into the material's behavior and performance under elevated temperatures, leading to the development of materials with enhanced mechanical properties, improved structural integrity, and increased resistance to crack propagation. These advancements contribute to the efficient, sustainable, and safe design and operation of marine infrastructure. In the future work, we will investigate the hybrid composite's long-term durability and environmental stability under marine conditions, including exposure to saltwater, UV radiation, and cyclic loading.

**Data availability** The data that support the findings of this study are available from the corresponding author upon reasonable request.

## Declarations

**Conflict of interest** The authors declare that they have no known competing financial interests or personal relationships that could have appeared to influence the work reported in this paper.

## References

1. S. Job, Composite hatch cover approved for use in commercial ship. Reinf. Plast. **2**, 58 (2015)
2. M. Abu-Okail, M. Nafea, M. Ghanem, M. El-Sheikh, A. El-Nikhaily, A. Abu-Oqail, Damage mechanism evaluation of polymer matrix composite reinforced with glass fiber via modified Arcan test specimens. J. Fail. Anal. Prev. **21**, 451–461 (2021)
3. D. Chalmers, Experience in design and production of FRP marine structures. Mar. Struct. **4**, 93–115 (1991)
4. M.O. Critchfield, T.D. Judy, A.D. Kurzweil, Low-cost design and fabrication of composite ship structures. Mar. Struct. **7**, 475–494 (1994)
5. M.H. Ata, M. Abu-Okail, G.M. Essa, T. Mahmoud, I. Hassab-Allah, Failure mode and failure load of adhesively bonded composite joints made by glass fiber-reinforced polymer. J. Fail. Anal. Prev. **19**, 950–957 (2019)
6. M. Abu-Okail, N.A. Alsaleh, W. Farouk, A. Elsheikh, A. Abu-Oqail, Y.A. Abdelraouf, M.A. Ghafaar, Effect of dispersion of alumina nanoparticles and graphene nanoplatelets on microstructural and mechanical characteristics of hybrid carbon/glass fibers reinforced polymer composite. J. Market. Res. **14**, 2624–2637 (2021)
7. C.A. Wood, W.L. Bradley, Determination of the effect of seawater on the interfacial strength of an interlayer E-glass/graphite/epoxy composite by in situ observation of transverse cracking in an environmental SEM. Compos. Sci. Technol. **57**, 1033–1043 (1997)
8. O.T. Bafakeeh, W.M. Shewakh, A. Abu-Oqail, W. Abd-Elaziem, M. Abdel Ghafaar, M. Abu-Okail, Synthesis and characterization of hybrid fiber-reinforced polymer by adding ceramic nanoparticles for aeronautical structural applications. Polymers **13**, 4116 (2021)
9. O.T. Bafakeeh, M.S. Shiba, A.B. Elshalakany, M. Abu-Okail, A.M. Hussien, Effect of dispersion hybrid structural properties of MWCNTs and $Al_2O_3$ on microstructural and thermal characteristics of PCMs for thermal energy storage in solar water desalination. J. Therm. Anal. Calorim. **148**, 4087–4104 (2023)
10. A.P. Mouritz, E. Gellert, P. Burchill, K. Challis, Review of advanced composite structures for naval ships and submarines. Compos. Struct. **53**, 21–42 (2001)
11. M. Meo, R. Vignjevic, G. Marengo, The response of honeycomb sandwich panels under low-velocity impact loading. Int. J. Mech. Sci. **47**, 1301–1325 (2005)
12. N.-Z. Chen, H.-H. Sun, C.G. Soares, Reliability analysis of a ship hull in composite material. Compos. Struct. **62**, 59–66 (2003)
13. P. Davies, Accelerated aging tests for marine energy applications, in *Durability of composites in a marine environment*. (Dordrecht, Springer, Netherlands, 2014), pp.165–177
14. J. Hoge, C. Leach, Epoxy resin infused boat hulls. Reinf. Plast. **60**, 221–223 (2016)

15. K.A. Feichtinger, Test methods and performance of structural core materials-IIA. Strain rate dependence of shear properties. Composites (Paris) **31**, 37–47 (1991)

16. B.E. Tawfik, H. Leheta, A. Elhewy, T. Elsayed, Weight reduction and strengthening of marine hatch covers by using composite materials. Int. J. Naval Archit. Ocean Eng. **9**, 185–198 (2017)

17. B. Polagye, J. Thomson, Screening for biofouling and corrosion of tidal energy device materials: in-situ results for admiralty inlet, puget sound, Washington, (2010)

18. M.H. Moosa, M. Abu-Okail, A. Abu-Oqail, S.A. Al-Shelkamy, W.M. Shewakh, M.A. Ghafaar, Structural and tribological characterization of carbon and glass fabrics reinforced epoxy for bushing applications safety. J. Polym. **15**, 2064 (2023)

19. S.A. Tekalur, K. Shivakumar, A. Shukla, Mechanical behavior and damage evolution in E-glass vinyl ester and carbon composites subjected to static and blast loads. Compos. B Eng. **39**, 57–65 (2008)

20. D.F. Hasson, C.R. Crowe, *Materials for marine systems and structures: treatise on materials science and technology*, vol. 28 (Elsevier, Amsterdam, 2013)

21. R. Olsson, Mass criterion for wave controlled impact response of composite plates. Compos. A Appl. Sci. Manuf. **31**, 879–887 (2000)

22. P. Davies, R. Baizeau, A. Wahab, S. Pecault, F. Collombet, and J.-L. Lataillade, Determination of material properties for structural sandwich calculations: from creep to impact loading. In Mechanics of Sandwich Structures: proceedings of the EUROMECH 360 Colloquium held in Saint-Étienne, France, 13–15 May 1997, pp. 327–336 (1998)

23. E. Gellhorn, G. Reif, Think dynamic--dynamic test data for the design of dynamically loaded structures. Engineering Materials Advisory Services Ltd. (United Kingdom), pp. 541–557 (1992)

24. A. Reza, H.M. Sedighi, Nonlinear vertical vibration of tension leg platforms with homotopy analysis method. Adv. Appl. Math. Mech. **7**, 357–368 (2015)

25. P. Rigo, E. Rizzuto, Analysis and design of ship structure. Ship Design Constr. **1**, 18–21 (2003)

26. A. Jensen, G. Havsgård, K. Pran, G. Wang, S. Vohra, M. Davis, A. Dandridge, Wet deck slamming experiments with a FRP sandwich panel using a network of 16 fibre optic Bragg grating strain sensors. Compos. B Eng. **31**, 187–198 (2000)

27. B. Hayman, J. Wedel-Heinen, P. Brøndsted, Materials challenges in present and future wind energy. MRS Bull. **33**, 343–353 (2008)

28. P. Davies, G. Germain, B. Gaurier, A. Boisseau, D. Perreux, Evaluation of the durability of composite tidal turbine blades. Phil. Trans. R. Soc. A **371**, 20120187 (2013)

29. C. Douglas, G. Harrison, J. Chick, Life cycle assessment of the Seagen marine current turbine. Proc. Inst. Mech. Eng. M J. Eng. Marit. Environ. **222**, 1–12 (2008)

30. M.A. Bashir, Use of dynamic mechanical analysis (DMA) for characterizing interfacial interactions in filled polymers. Solids **2**, 108–120 (2021)

31. S. Ravi, K. Saravanan, D. Jayabalakrishnan, P. Prabhu, V. Suyamburajan, V. Jayaseelan, A. Mayakkannan, Silane grafted nanosilica and aramid fibre-reinforced epoxy composite: dma, fatigue and dynamic loading behaviour. SILICON (2021). https://doi.org/10.1007/s12633-021-01060-0

32. A. Redmann, M.C. Montoya-Ospina, R. Karl, N. Rudolph, T.A. Osswald, High-force dynamic mechanical analysis of composite sandwich panels for aerospace structures. Compos. C Open Access **5**, 100136 (2021)

33. M. Alsaadi, M. Bulut, A. Erkliğ, A. Jabbar, Nano-silica inclusion effects on mechanical and dynamic behavior of fiber reinforced carbon/Kevlar with epoxy resin hybrid composites. Compos. B Eng. **152**, 169–179 (2018)

34. B. Muralidhara, S.K. Babu, B. Suresha, Studies on the role of graphene nanoplatelets on mechanical properties, dynamic-mechanical and thermogravimetric analysis of carbon-epoxy composites. J. Inst. Eng. India Ser. D (2020). https://doi.org/10.1007/s40033-020-00219-0

35. W. Li, D. He, J. Bai, The influence of nano/micro hybrid structure on the mechanical and self-sensing properties of carbon nanotube-microparticle reinforced epoxy matrix composite. Compos. A Appl. Sci. Manuf. **54**, 28–36 (2013)

36. W.G. McDonough, J. Dunkers, K. Flynn, D. Hunston, A test method to determine the fiber and void contents of carbon/glass hybrid composites. J. ASTM Int. **1**, 1–15 (2004)

37. A. Shrivastava, Plastic properties and testing, in *Introduction to plastics engineering*. (Elsevier, Amsterdam, 2018), pp.49–110

38. P.J. Trzebiatowska, A.S. Echart, T.C. Correas, A. Eceiza, J. Datta, The changes of crosslink density of polyurethanes synthesised with using recycled component. Chemical structure and mechanical properties investigations. Prog. Org. Coat. **115**, 41–48 (2018)

39. W. Ji, L. Zhang, Diamond nanothread reinforced polymer composites: ultra-high glass transition temperature and low density. Compos. Sci. Technol. **183**, 107789 (2019)

40. N. Baral, D.D. Cartié, I.K. Partridge, C. Baley, P. Davies, Improved impact performance of marine sandwich panels using through-thickness reinforcement: experimental results. Compos. B Eng. **41**, 117–123 (2010)

41. A. Shrivastava, *Introduction to plastics engineering* (William Andrew, Norwich, 2018)

42. N.I.N. Haris, M.Z. Hassan, R. Ilyas, M.A. Suhot, S. Sapuan, R. Dolah, R. Mohammad, M. Asyraf, Dynamic mechanical properties of natural fiber reinforced hybrid polymer composites: a review. J. Mater. Res. Technol. (2022). https://doi.org/10.1016/j.jmrt.2022.04.155

43. K. Karvanis, S. Rusnáková, M. Žaludek, A. Čapka, Preparation and dynamic mechanical analysis of glass or carbon fiber/polymer composites. In IOP Conference Series: materials science and engineering, p. 012005 (2018)

44. A. Merzoug, B. Bouhamida, Z. Sereir, A. Bezazi, A. Kilic, Z. Candan, Quasi-static and dynamic mechanical thermal performance of date palm/glass fiber hybrid composites. J. Ind. Text. **51**, 7599S-7621S (2022)

45. A. Atiqah, M. Jawaid, S. Sapuan, M. Ishak, Dynamic mechanical properties of sugar palm/glass fiber reinforced thermoplastic polyurethane hybrid composites. Polym. Compos. **40**, 1329–1334 (2019)

46. N. Jesuarockiam, M. Jawaid, E.S. Zainudin, M. Thariq Hameed Sultan, R. Yahaya, Enhanced thermal and dynamic mechanical properties of synthetic/natural hybrid composites with graphene nanoplateletes. Polymers **11**, 1085 (2019)

47. Z. Kamble, B.K. Behera, R. Mishra, P.K. Behera, Influence of cellulosic and non-cellulosic particle fillers on mechanical, dynamic mechanical, and thermogravimetric properties of waste cotton fibre reinforced green composites. Compos. B Eng. **207**, 108595 (2021)

48. I.M. Alarifi, A performance evaluation study of 3d printed nylon/glass fiber and nylon/carbon fiber composite materials. J. Market. Res. **21**, 884–892 (2022)

49. A. Ari, A. Bayram, M. Karahan, S. Karagöz, Comparison of the mechanical properties of chopped glass, carbon, and aramid fiber reinforced polypropylene. Polym. Polym. Compos. **30**, 09673911221098570 (2022)

50. Z. Xu, A. Nakai, Y. Yang, H. Hiroyuki, A study on the initial fracture behavior of CF/GF intra-hybrid woven fabric reinforced composites. Open J. Compos. Mater. **8**, 11–27 (2017)

## Authors and Affiliations

**Mohamed Abu-Okail[1] · Metwally Abdel Ghafaar[1] · Abou Bakr Elshalakany[2,3] · Mohamed S. Shiba[4] · Ahmed Abu-Oqail[5] · Mohammed Gamil[6]**

✉ Mohamed Abu-Okail
  MohamedAbuOkail@gmail.com

[1] Manufacturing Engineering and Production Technology Department, Modern Academy for Engineering and Technology, Cairo 11571, Egypt

[2] Production Engineering and Printing Technology Department, Akhbar El Yom Academy, Giza 12451, Egypt

[3] Faculty of Energy and Industrial Technology, October Technological University, Giza, Egypt

[4] Automotive Engineering Department, Higher Technological Institute, 10th of Ramadan City, 6th of October Branch, Giza 12622, Egypt

[5] Mechanical Production Department, Faculty of Technology and Education, Beni-Suef University, Beni-Suef, Egypt

[6] Department of Mechanical Engineering, Faculty of Engineering at Shoubra, Benha University, Cairo 11629, Egypt